Crystal Structure of a Human Cyclin-Dependent Kinase 6 Complex with a Flavonol Inhibitor, Fisetin

Heshu Lu,[†] Debbie J. Chang,[‡] Blandine Baratte,[§] Laurent Meijer,[§] and Ursula Schulze-Gahmen*,[†]

Physical Biosciences Division at Lawrence Berkeley National Laboratory, 1 Cyclotron Road, MS 64R0121, Berkeley, California 94720, and Station Biologique de Roscoff, C.N.R.S., BP 74, 29682 Roscoff Cedex, Bretagne, France

Received August 6, 2004

Cyclin-dependent kinases (CDKs) play a central role in cell cycle control, apoptosis, transcription, and neuronal functions. They are important targets for the design of drugs with antimitotic or antineurodegenerative effects. CDK4 and CDK6 form a subfamily among the CDKs in mammalian cells, as defined by sequence similarities. Compared to CDK2 and CDK5, structural information on CDK4 and CDK6 is sparse. We describe here the crystal structure of human CDK6 in complex with a viral cyclin and a flavonol inhibitor, fisetin. Fisetin binds to the active form of CDK6, forming hydrogen bonds with the side chains of residues in the binding pocket that undergo large conformational changes during CDK activation by cyclin binding. The 4-keto group and the 3-hydroxyl group of fisetin are hydrogen bonded with the backbone in the hinge region between the N-terminal and C-terminal kinase domain, as has been observed for many CDK inhibitors. However, CDK2 and HCK kinase in complex with other flavone inhibitors such as quercetin and flavopiridol showed a different binding mode with the inhibitor rotated by about 180°. The structural information of the CDK6−fisetin complex is correlated with the binding affinities of different flavone inhibitors for CDK6. This complex structure is the first description of an inhibitor complex with a kinase from the CDK4/6 subfamily and can provide a basis for selecting and designing inhibitor compounds with higher affinities and specificities.

Introduction

The mammalian cell cycle consists of four stages: S phase (S) where DNA synthesis occurs, mitosis (M) during which the actual cell division takes place, and two gap phases (G1 and G2) during which required cell components are synthesized and assembled. The progression of cells through G1 phase and the G1/S transition is regulated by cyclin-dependent kinase 4 and 6 complexes with cyclinD and CDK2 in complex with cyclinE,[1] whereas the transition through S phase and mitosis is regulated by CDK1 and CDK2 in complex with cyclinA and cyclinB. The inactive CDK apoenzymes are partially activated by complex formation with regulatory cyclin subunits. The CDK−cyclin complexes are further activated by phosphorylation of a threonine residue (Thr 160^{CDK2}, Thr 177^{CDK6}) in the activation loop (T-loop), which spans residues Asp 163^{CDK6} to Glu 189^{CDK6}.[2] In addition, CDK activity is regulated by dephosphorylation on a threonine and a tyrosine residue (Thr14, Tyr 15 in CDK2; Tyr 24 in CDK6), by intracellular distribution, and by complex formation with CDK inhibitors (CDKIs) of the CIP/KIP and INK type.[3] Appropriate cell cycle regulation is essential for the control of cell proliferation, and mutations or alterations in the expression levels of CDK regulators are frequently found in cancer.[4−9]

Due to their key role in cell cycle control and neuronal functions, CDKs have been an important target for the design of drugs for treatment of the pathogenic effects of tumorigenesis and neurodegenerative diseases.[10−15] A number of quite specific and high-affinity inhibitors of CDK2 have been identified in recent years, including olomoucine, roscovitine, purvalanol, CVT-313, toyocamycin, flavopiridol, and others.[11] However, only three types of semispecific CDK4 inhibitors have been described, a benzocarbazole, an aminothiazole, and a pyrimidine derivative.[10] CDK4 and CDK6 form a subgroup within the CDKs. They are 70% identical between each other but only about 45% identical with other CDKs. CDK1, CDK2, and CDK5 are structurally very similar, and many inhibitors of these enzymes are inactive on CDK4 and CDK6.[14]

Drug design of the CDK2-specific inhibitors was largely helped by iterative cycles of CDK2−inhibitor complex structure determinations and structure-based drug design. For example, the initial already specific inhibitor olomoucine had an IC_{50} value of 7000 nM for CDK2. Modifications of this inhibitor were suggested based on the complex structure of CDK2 and olomoucine. The second and third generation inhibitors roscovitine and purvalanol A/B had IC_{50} values of 450 and 4 nM, respectively.[15]

Because CDK6 and CDK4 control the entrance into the cell cycle, they are especially interesting for pharmacological intervention and as tools for cell cycle research. The structure of an active CDK6 complex with a virus-encoded cyclin from herpesvirus saimiri (Vcyclin) was recently determined to 3.1 Å resolution.[16] We describe here the first complex structure of human CDK6 with a small molecule inhibitor, fisetin (3,7,3′,4′-tetrahydroxyflavone) to 2.9 Å resolution. Fisetin inhibits CDK6 with an IC_{50} value of 0.85 μM. The binding

* Author to whom correspondence should be addressed. Phone: (510) 486-5854. Fax: (510) 486-6798. E-mail: uschulze-gahmen@lbl.gov.
[†] Lawrence Berkeley National Laboratory.
[‡] Currently at Department of Molecular Pharmacology, Stanford University, Stanford, CA 94305-5441.
[§] Station Biologique de Roscoff.

10.1021/jm049353p CCC: $30.25
Published on Web 01/20/2005

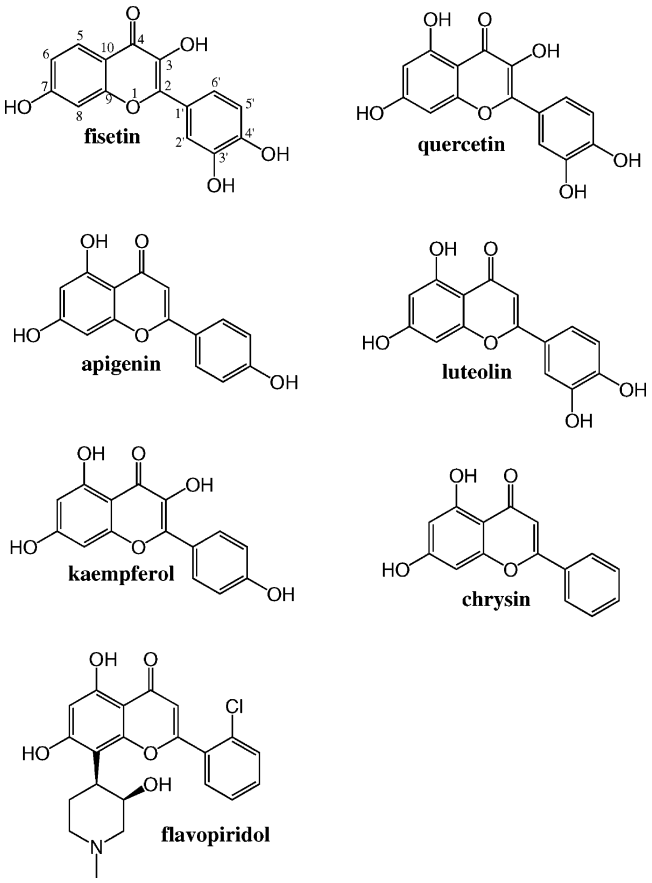

Figure 1. Molecular structure of seven flavone inhibitors of protein kinases, fisetin, quercetin, apigenin, luteolin, kaempferol, chrysin, and flavopiridol.

affinities of six related flavone inhibitors were determined as well and are discussed with reference to the complex structure of CDK6 with fisetin. The structural information from the CDK6−fisetin complex will be valuable in designing improved inhibitor molecules with specificity for CDK6 or CDK4.

Results and Discussion

Overall Structure of the Complex. The crystal structure of CDK6−Vcyclin has been described recently.[16] Here, we describe the structure of the same enzyme in complex with a flavonol inhibitor, 3,7,3′,4′-tetrahydroxyflavone or fisetin (Figures 1 and 2). Compared to the native structure, the fisetin complex structure is a better defined structure. The resolution of the complex structure, at 2.9 Å, is higher than that of the native structure, and some previously undefined regions can now be traced in the complex. There are still a few areas with undefined electron density for residues 1−10, 88−90, and 256−258 in CDK6 and 1−8 and 124−126 in Vcyclin. However, the key elements of the structure are well-defined in the electron density map, including the PLSTIRE helix (α1), the unphosphorylated T-loop, which contains the potential phosphorylation site Thr177, and the fisetin binding pocket. The final CDK6−Vcyclin−fisetin structure has an R_{factor} of 26.0% (R_{free} = 31.3%) at 2.9 Å with good stereochemistry (Table 1).

As expected from the same space group and similar cell dimensions of the inhibitor complex and the native complex, we observe very similar backbone conformations in both structures. CDK6, in common with other kinases, consists of two domains, with the smaller N-terminal domain rich in β-sheet structure (residues 1−100) and the larger, mostly α-helical, C-terminal domain (residues 101−308). Fisetin was found to bind in the ATP-binding pocket, which is located between the two kinase domains (Figure 2). The Vcyclin subunit consists of two domains, each adopting the typical cyclin fold. The relative orientation of Vcyclin and CDK6 domains in the fisetin complex is very similar to that in the native structure. (Figure 2). The root mean square (rms) deviations on Cα atoms in CDK6 between the fisetin complex and the native one is 0.781 Å, with 0.569 Å for the Cα atoms in the kinase C-terminal domain and 0.770 Å in the kinase N-terminal domain. Larger local differences are found in peptide segments that are located at chain termini or in loops on the surface of the molecule. These flexible residues were excluded from the calculation of rms deviations on Cα atoms.

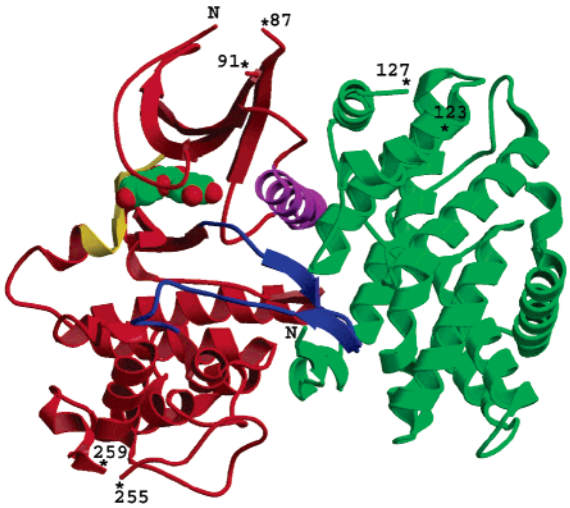

Figure 2. Schematic drawing of the CDK6−Vcyclin complex with bound fisetin inhibitor. CDK6 is shown in red with the PLSTIRE helix in purple, the T-loop in blue, and the hinge region in yellow. Cyclin is shown in green. Missing regions in the protein are labeled with stars and residue numbers at the chain interruptions. Fisetin is shown as a CPK model bound in the ATP binding pocket of the kinase.

Structure of the Ligand-Binding Pocket with Bound Fisetin. The $F_o - F_c$ electron density map for the CDK6−Vcyclin−fisetin complex after rigid-body refinement shows clear density for all atoms of fisetin (Figure 3A). Fisetin binds in the ATP-binding pocket of CDK6, which is formed between the N- and C-terminal domains of the enzyme (Figure 3C). The fisetin binding mode was confirmed by calculating difference maps for two possible inhibitor orientations. The difference map for the inhibitor orientation with the dihydroxyphenyl group pointing into the binding pocket (orientation I) is flat with a few random noise peaks, whereas the difference map for the 180° rotated orientation (orientation II) shows a strong positive peak (2.5 σ) for the 3′ hydroxyl group of orientation I and two negative peaks in the 3′ and 4′ hydroxyl positions of orientation II (Figure 3B). Hence, orientation I is the correct orientation. As seen for almost all other CDK inhibitors, fisetin in orientation I is anchored in the binding pocket by the formation of a pair of hydrogen bonds between the 3-hydroxyl and 4-keto group of fisetin and the carbonyl

Table 1. Data Collection and Refinement Statistics

Data Collection			
resolution range (Å)	50−2.9	average I/σ_I[a]	18.6 (4.4)
no. of observations	107 223	R_{sym} (%)[a,b]	11.7 (53.8)
no. of unique reflections	12 984	mosaicity	0.69
completeness (%)[a]	91.4 (90.0)		
Refinement			
resolution (Å)	20−2.9	Ramachandran analysis (%)	
data/parameter	0.78	most favored[e]	80.6
R_{cryst}[c]/R_{free}[d]	0.260/0.313	addition allowed	17.3
no. of atoms	4173	generously allowed	2.1
CDK6	2241	disallowed	0
Vcyclin	1911	average B-factor (Å^2)	58.8
fisetin	21	CDK6	65.8
rms deviations		Vcyclin	50.9
bond (Å)	0.008	fisetin	26.6
angles (deg)	1.38		

[a] Values in parentheses refer to the highest resolution shell. [b] $R_{sym} = \Sigma_h\Sigma_i\ |I_{h,i} - I_h|/\Sigma_h\Sigma_i\ I_{h,i}$ for the intensity (I) of i observation of reflection h. [c] $R_{cryst} = \Sigma_h||F_{obs}(h)| - |F_c(h)||/\Sigma_h|F_{obs}(h)|$ for all data. [d] R_{free} was calculated for 7.5% of structure factor amplitudes excluded from refinement. [e] Most favored region in Ramachandran plot as defined in PROCHECK[24].

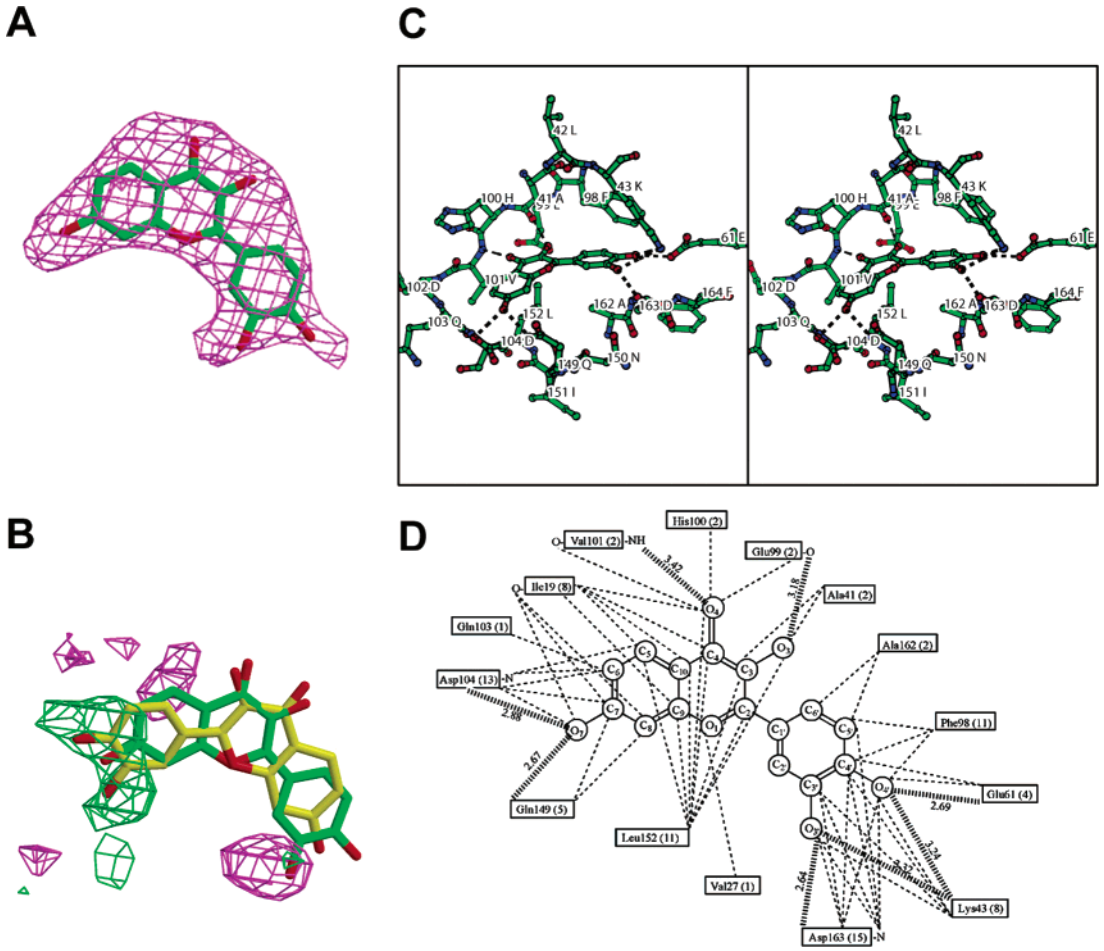

Figure 3. Schematic drawings of fisetin interactions with residues in the CDK6 binding pocket. (A) Electron density for the bound inhibitor. The $\alpha_{calc}(|F_o| - |F_c|)$ simulated annealing omit map was calculated to 2.9 Å resolution and contoured at 3σ. (B) Difference electron density map for fisetin bound in the rotated orientation II. The map was contoured at 2.5σ (purple) and −2.5σ (green). The fisetin model in orientation I is shown in green, the fisetin model in orientation II in yellow. (C) Stereoview of fisetin interactions with residues in the CDK6 binding pocket. Hydrogen bonds are shown as broken lines. (D) Schematic of CDK6 interactions with fisetin. Protein residues are shown as rectangular boxes labeled with the residue number and the total number of contacts in brackets. Side-chain contacts are indicated by lines connecting to the respective residue box, and interactions to main-chain atoms are shown as lines to the specific main-chain atoms. Van der Waals contacts are indicated as broken lines and hydrogen bonds by dashed lines.

oxygen of Glu99^{CDK6} and the amide nitrogen of Val101^{CDK6}, respectively. The inhibitor is bound in such an orientation that the 3′,4′-dihydroxyphenyl group of fisetin points into the binding pocket occupying the part of the binding pocket where the α-phosphate of ATP would bind. In this orientation, the 4′-hydroxyl group of fisetin can form hydrogen bonds with Lys43^{CDK6} and Glu61^{CDK6}, and the 3′ hydroxyl group forms a hydrogen bond with Asp163^{CDK6}. All three of these CDK6 residues are essential for the catalytic activity of eukaryotic

Table 2. Intermolecular Contacts between CDK6 and Fisetin[a]

CDK6 residue (CDK2 residue)	total contacts (<4.11Å)	hydrogen bond with fisetin atom
Ile19 (Ile10)	8	
Val27 (Val8)	1	
Ala41 (Ala31)	2	
Lys43 (Lys33)	8	1 with 3′OH,1 with 4′OH
Glu61 (Glu51)	4	1 with 4′OH
Phe98 (Phe80)	11	
Glu99 (Glu 81)	2	1 with 3 OH
His100 (Phe82)	2	
Val101 (Leu83)	2	1 with 4 O
Gln103 (Gln85)	1	
Asp104 (Asp86)	13	1 with 7 OH
Glu149 (Gln131)	5	1 with 7 OH
Leu152 (Leu134)	11	
Ala162 (Ala144)	2	
Asp163 (Asp145)	15	1 with 3′OH
total number	87	8

[a] Contacts are grouped into those with residues in the N-terminal domain (upper section), those with residues in the hinge region (middle section), and those with residues in the C-terminal domain (bottom section).

protein kinases.[17] Glu61^{CDK6} is located in the α1-helix of the N-terminal domain, which changes its orientation during the activation of CDKs by cyclin binding.[18] As a result, the side chain of Glu61 points away from the ATP-binding pocket in the apoenzyme but points into the binding pocket in the activated enzyme. Because fisetin forms a buried hydrogen bond with Glu61, it appears likely that the inhibitor will bind with lower affinity to the inactive apoenzyme than to the activated enzyme conformation seen in this structure. Fisetin is the first CDK inhibitor that has been reported to form hydrogen bonds with Glu61 in the PLSTIRE helix.

In general, fisetin binds more extensively to the C-terminal domain than to the N-terminal domain (Table 2). A total of 87 interatomic contacts, including 8 hydrogen bonds, are formed between CDK6 and fisetin. Of these contacts, 47 are with the benzopyran ring and 40 with the phenyl ring (Figure 3D, Table 2). The relatively large number of contacts with the dihydroxyphenyl ring reflects the close shape complementarity of the binding pocket for this part of the inhibitor. The hydrophobic core of the benzopyran ring makes numerous favorable van der Waals contacts with the backbone and side chains of residues 99 to 104 from the hinge area connecting the two CDK6 domains and with Gln149 and Leu152 from the C-terminal domain (Figure 3, parts C and D). In addition to the hinge anchoring hydrogen bonds with the 3-hydroxyl group and 4-keto group, the 7-hydroxyl group of fisetin is in a position to form hydrogen bonds with the side chains of Asp104^{CDK6} and Gln149^{CDK6}.

Structural differences in the ligand-binding pocket between CDK6−Vcyclin and its complex with fisetin are minor. Although structural changes in the backbone structure are insignificant at 2.9 Å resolution, small changes in the orientation of several side chains are observed that lead to a better fit between fisetin and CDK6. The side chains of residues Lys43^{CDK6}, Glu61^{CDK6}, Phe98^{CDK6}, His100^{CDK6}, Asp104^{CDK6}, and Asp163^{CDK6} show small adjustments in the order of 0.5 to 2.0 Å in the position of side-chain atoms.

A comparison of the CDK6−fisetin complex structure with the structure of a related complex between the CDK2 apoenzyme and another flavone inhibitor, deschloro-chloroflavopiridol,[19] shows a different binding mode for the inhibitors. Fisetin appears flipped by 180° around the short axis of the benzopyran ring system relative to the bound flavopiridol in the CDK2-complex structure. The flipping changes the orientation of the 3′,4′-dihydroxyphenyl group from being positioned at the opening of the binding pocket in the flavopiridol complex to being deeply buried in the binding pocket where the hydroxyl groups form hydrogen bonds with several of the catalytic kinase residues (Figure 4) in the fisetin complex. These different binding orientations agree with previous reports of various binding modes of related

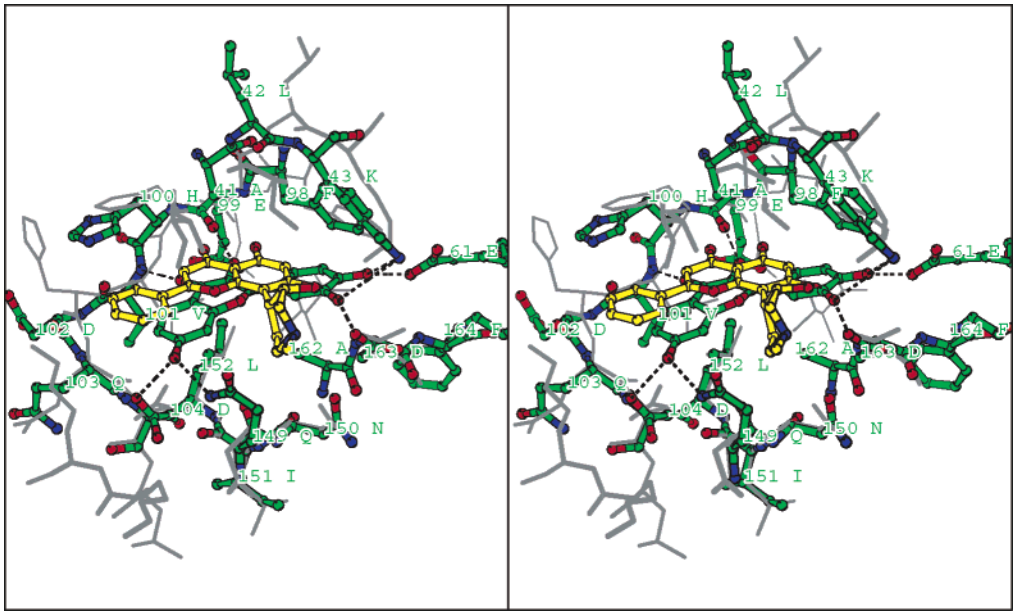

Figure 4. Comparison of the binding pockets of the CDK6−fisetin complex and the CDK2−deschloro-flavopiridol complex. The CDK6−fisetin complex is shown in green. Deschloro-flavopiridol is shown in yellow, and CDK2 in gray. The kinases were superimposed on the C-terminal kinase domains. Residue labels are shown for CDK6.

Table 3. Kinase Inhibition of Various Flavonoid Inhibitors[a]

	CDK6/Vcyclin	CDK5/p25	CDK1/cyclinB	GSK-3[b]
fisetin	0.85	0.57	0.79	0.42
apigenin	1.7	1.6	4.0	1.4
luteolin	> 300	3.8	6.2	0.8
quercetin	25	23	75	2.1
chrysin	6	3.1	7.1	7.2
kaempferol	22	51	41	3.5
flavopiridol	0.08	0.17	0.21	0.28

[a] Enzyme activities were assayed as described in the Experimental Section, in the presence of increasing concentrations of inhibitor. IC_{50} values were calculated from the dose−response curves and are presented in micromolar. [b] Glycogen synthase kinase-3.

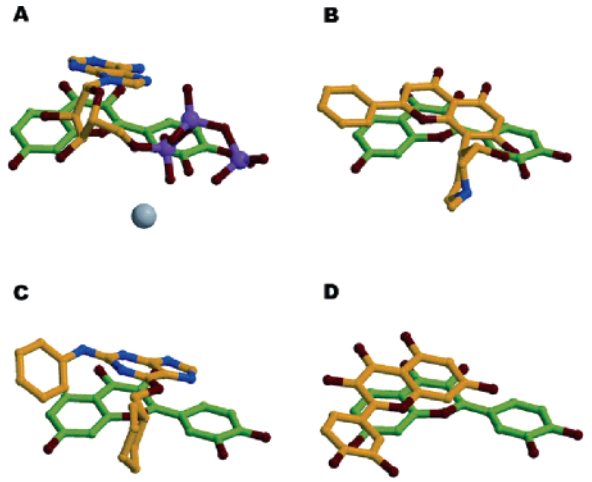

Figure 5. Comparison of the binding mode of various CDK ligands and inhibitors. All kinase complexes were superimposed on the C-terminal kinase domain using the program Overlap.[29] Fisetin from the CDK6−fisetin complex is shown in green. Superimposed are four other ligands shown in yellow, (A) CDK2−ATP,[30] (B) CDK2−deschloro-flavopiridol,[19] (C) CDK2−NU6094,[31] and (D) HCK−quercetin.[20] The Mg atom coordinated to ATP in (A) is shown in gray.

CDK inhibitors. The hydrophobic ATP-binding pocket seems to be able to accommodate a large variety of hydrophobic inhibitors in different orientations.

Correlation of Structural Results with Binding Affinities. To get a better understanding for the different binding affinities of related flavone inhibitors to CDK6−Vcyclin (Figure 1, Table 3), we analyzed the different IC_{50} values for the inhibitors with reference to the CDK6−Vcyclin−fisetin complex structure and other complex structures between flavone inhibitors and protein kinases. Complex structures of flavopiridol and quercetin with CDK2 [19] and the src-family HCK kinase,[20] respectively, showed that these inhibitors can bind in an orientation that is roughly 180° rotated about the bond joining the two ring systems of the benzopyrane structure relative to the fisetin−CDK6 complex (Figure 5, parts B and D). In this orientation, the phenyl ring points to the outside of the ATP-binding pocket. In both orientations, the oxygen of the keto group forms a hydrogen bond with the backbone amide group of $Leu83^{CDK2}$ or its equivalent in the hinge region, and the hydroxyl groups in position 3 or 5 form additional hydrogen bonds with backbone atoms in the hinge region. The more favorable orientation for each inhibitor−kinase complex may depend on the specific combination of hydroxyl groups on the benzopyran ring as well as on substituents in the phenyl group that might lead to steric hindrances or provide favorable contacts in one versus the other orientation. In the CDK6−fisetin complex, the 4′-hydroxyl group on the phenyl ring forms a buried hydrogen bond with $Glu61^{CDK6}$ that may contribute to the preferred orientation with the phenyl ring buried in the pocket. Apigenin binds with very similar affinity to CDK6 as fisetin (IC_{50} values of 1.7 μM for apigenin and 0.85 μM for fisetin). The only differences in the chemical structure of apigenin compared to fisetin are the absence of hydroxyl groups in the 3- and 3′-positions and an added hydroxyl group in the 5-position of the benzopyrane ring. Superposition of the apigenin structure on the fisetin−CDK6 complex shows that a 5-hydroxyl group should be able to form a hydrogen bond with the carbonyl oxygen of $Val101^{CDK6}$. Hence, the loss of the hydrogen bond with the 3-hydroxyl group might be partially compensated by a new hydrogen bond with the 5-hydroxyl group. The loss of the hydrogen bond between the 3′-hydroxyl group in the phenyl ring and $Asp163^{CDK6}$ does not appear to affect the binding affinity much, which may be due to the solvent-exposed nature of the bond. Chrysin binds with 7-fold lower affinity than fisetin. Its molecular structure resembles apigenin without the hydroxyl group on the phenyl ring. It can also be viewed as a substructure of deschloro-flavopiridol. Its similarity with deschloro-flavopiridol suggests that chrysin would bind in the rotated-binding mode described in the CDK2−deschloro-flavopiridol complex structure.[19]

Fisetin, quercetin, kaempferol, and luteolin are even more similar in their chemical structures (Figure 1). Addition of one more hydroxyl group in the 5-position of the benzopyran ring will give quercetin, and a simultaneous removal of the 3′-hydroxyl group will result in kaempferol. Addition of the 5-hydroxyl plus removal of the 3-hydroxyl group will give luteolin. The IC_{50} values for quercetin, kaempferol, and luteolin are 30, 26, and >350 times higher than that for fisetin. Replacement of fisetin with quercetin, kaempferol, or luteolin in the complex structure shows a good fit for the inhibitors. The additional 5-hydroxyl group would be in a position to form a hydrogen bond with the backbone carbonyl group of $Val101^{CDK6}$, and there do not seem to be any unfavorable contacts. The missing 3-hydroxyl group in luteolin would leave the carbonyl oxygen of $Glu99^{CDK6}$ without a hydrogen-bonding partner, and there would be an unfilled pocket in the binding site. The superposition of the three inhibitors onto the fisetin complex structure does not easily explain why quercetin, kaempferol, and luteolin bind with lower affinity to CDK6 than fisetin. It could be that the hydrogen bond between the 5-hydroxyl of the benzopyrane ring and the hinge region will lead to a small change in the orientation of the inhibitor, which could cause unfavorable contacts for the dihydroxyphenyl group that is bound in a fairly tight fitting pocket in the fisetin complex. Alternatively, the inhibitor might bind in the rotated mode described earlier for the flavopiridol−CDK2 complex and the HCK−quercetin complex, which would lead to a completely different set of interactions.

Conclusion

The complex structure of CDK6−Vcyclin with the inhibitor fisetin is the first inhibitor complex structure

with a kinase from the CDK subfamily consisting of CDK4 and CDK6. Fisetin is a relatively small flavonol inhibitor with a hydroxyl group in the 3-position of the benzopyran ring. This distinguishes it from several other flavone inhibitors whose inhibitory activity on CDK6−Vcyclin was determined in this study as well (Table 3). Flavopiridol, luteolin, apigenin, and chrysin have a hydroxyl group in the 5-position of the benzopyran ring, whereas quercetin and kaempferol have hydroxyl groups in the 3- and 5-positions. The different positions of the hydroxyl groups may lead to different orientations of the bound inhibitors as seen for the CDK2−flavopiridol complex versus the CDK6−fisetin complex (Figure 4). Fisetin binds with the dihydroxyphenyl group buried deep in the ATP-binding pocket, close to $Phe98^{CDK6}$ with the 4′-hydroxyl hydrogen bonded to two catalytic residues, $Lys43^{CDK6}$ and $Glu61^{CDK6}$. Because these residues undergo a large conformational change during activation of CDK6 by cyclin binding, it is likely that fisetin binds with higher affinity to the activated form of CDK6 than to the inactive apoenzyme. Bound fisetin is almost completely buried in the ATP-binding pocket of CDK6 with 232 and 344 Å^2 buried surface area for fisetin and CDK6, respectively. Hence, it is not surprising that fisetin inhibits CDKs and probably other kinases nonspecifically. To increase the specificity and the affinity of a fisetin-based inhibitor, additional substituent groups may need to be added to the scaffold. An overlap of fisetin with other CDK inhibitors with higher affinity (Figure 5, parts B and C) show in several cases an additional group that can bind in the ribose or α-phosphate binding pocket. Adding a substituent in the 2′-position of the dihydroxyphenyl ring of fisetin may create a ligand that is better able to fill this pocket and bind with higher affinity to CDK6. Higher inhibitor specificity is dependent on interactions with less conserved parts of the binding pocket. For CDKs, the less-conserved residues are located in the hinge or linker between the N-terminal and C-terminal kinase domains. Exploring substitutions in the 6- and 7-positions of the benzopyran ring may yield a more specific inhibitor for CDK6 by forming contacts with less-conserved residues in the hinge region. Increasing the structural information on CDK6−inhibitor complexes is important to get a better understanding of the structural basis of CDK-specific inhibitors, in particular CDK4/6-specific inhibitors which will in turn help to design more specific inhibitory compounds.

Experimental Section

Inhibitors. Fisetin, (3,7,3′,4′-tetrahydroxyflavone), $C_{15}H_{10}O_6$, $M_w = 286.24$, was purchased from Indofine Chemical Company (Somerville, NY). It was prepared as 50 mM stock solutions in ethanol for use in cocrystallization. Luteolin was a gift from Dr. G. R. Pettit (Arizona State University). It was purified from the medicinal plant *Terminalia arjuna*.[21] Quercetin, apigenin, kaempferol, and chrysin were obtained from Sigma.

Protein Expression and Purification. A complex of human CDK6 and Vcyclin was prepared as described.[22] In brief, Sf9 insect cells were infected with recombinant baculovirus containing the human CDK6 gene or a His-tagged Vcyclin gene. The CDK6-infected Sf9 cells and Vcyclin-infected Sf9 cells were lysed separately. The supernatants were combined, centrifuged for 75 min at 300 000*g*, and purified over a 7 mL Talon column (BD Biosciences Clontech, Palo Alto, CA) followed by a 7 mL Source Q ion-exchange column (Amersham Bioscience, Piscataway, NJ). After cleavage of the N-terminal His tag from Vcyclin with recombinant tobacco etch virus protease, the pure CDK6−Vcyclin complex was repurified over a 7 mL Source Q column.

Kinase Assays. To assay inhibitor activities on CDK6, a filter-binding assay was established. The following are combined in the reaction mixture: 2 μL of CDK6 (0.7 mg/μL), 5 μL of histone H1 (6 mg/mL), 14 μL of kinase buffer (60 mM β-glycerophosphate, 30 mM *p*-nitrophenyl phosphate, 25 mM MOPS (pH 7.0), 5 mM EGTA, 15 mM $MgCl_2$, 1 mM DTT, 0.1 mM Na−vanadate), 3 μL of inhibitor diluted in 50% DMSO, and 6 μL of ^{33}P-ATP (1 mCi/mL) in nonradioactive ATP at 90 μM concentration (final concentration: 15 μM). The assay is initiated by the addition of ^{33}P-ATP. The reaction is incubated for 20 min at 30° C. A 25 μL aliquot of the supernatant is then spotted onto Whatman P81 phosphocellulose paper. Filters are washed 5 times with 1% phosphoric acid solution. Wet filters are counted in the presence of 1 mL of scintillation fluid. Kinase activity is expressed as a percentage of maximal activity (without inhibitor).

Inhibitor Cocrystallization and Data Collection. We cocrystallized the CDK6−Vcyclin−fisetin complex under similar conditions as the uncomplexed CDK6−Vcyclin complex.[22] The purified protein was concentrated to 10 mg/mL in 25 mM Tris-HCl pH 8.0, 150 mM NaCl, 10 mM DTT, and 0.5 mM EDTA for crystallization experiments using the hanging-drop vapor-diffusion method. Fisetin was added to the CDK6−Vcyclin solution at a final concentration of 1 mM and preincubated for 4 h at 4 °C. This mixture was combined in a 1:1 (v/v) ratio with the precipitant, 50 mM Tris/HCl pH 8.0, 0.1 M CaOAc, 10% PEG 3350, 10 mM DTT. Sulfo-betaine 201 was added to the crystallization drop to a final concentration of 0.1 M, and the drop was equilibrated against the precipitant at 22 °C. Hexagonal plate-shaped crystals with an average size of $0.1 \times 0.1 \times 0.04$ mm^3 appeared after 1−3 days.

A complete data set from a complex crystal was collected at the Advance Light Source (Lawrence Berkeley National Laboratory) beamline 5.01 on a Quantum 2×2 array CCD detector (Area Detector Systems Corporation). A total rotation range of 70° was collected with 0.2° rotation per frame at a distance of 250 mm and a wavelength of 1.0 Å. Under these conditions, the crystals diffracted to 2.8 Å. The data were processed with HKL2000.[23] Autoindexing and examination of systematic absences indicated that the space group is $P6_522$, the same as the native one, with unit cell parameters $a = b = 66.2$ Å, $c = 448.47$ Å, $\gamma = 120°$ and one complex per asymmetric unit (Table 1).

Structure Determination and Model Refinement. The structure of the CDK6−Vcyclin−fisetin complex was solved by molecular replacement, using the structure of CDK6−Vcyclin as a model.[16] The model was placed in the asymmetric unit using AmoRe.[24] In the following rigid-body refinement, the R_{factor} decreased from 43.3% to 37.0% for the data between 9 and 3.0 Å. At this stage $F_o - F_c$ maps were calculated. These maps showed clear density for inhibitor bound to the ATP-binding pocket of CDK6. The conformation of residues forming the ATP-binding pocket was checked in simulated annealing, omit maps before the inhibitor molecule was included in the complex structure. Further refinement in CNS[25] continued with simulated annealing using the slow-cooling protocol, followed by alternate cycles of conjugate gradient minimization refinement in CNS and manual rebuilding using O.[26]

Protein superpositions and root-mean-square (rms) deviations on Cα atoms were done with the program LSQKAB from CCP4.[24] Hydrogen bonds and van der Waals contacts were assigned with the program CONTACT.[27] The cutoff for hydrogen bonds and salt bridges was 3.4 Å and up to 4.11 Å for van der Waals contacts, depending on the atom type and using standard van der Waals radii. Buried surface areas were calculated with the program MS[28] and a 1.4 Å probe radius.

Coordinates. Coordinates of the model and structure factors have been deposited in the Protein Data Bank (accession code 1XO2).

Acknowledgment. We thank Dr. G. R. Pettit for providing us with luteolin and O. Lozach for the assays performed with luteolin. We thank the staff at the ALS, Berkeley, CA, who provided excellent facilities for data collection. This research was supported by a grant from the National Institutes of Health (U.S.G.), by the "Association pour la Recherche sur le Cancer" (L.M.), and by the Ministère de la Recherche/INSERM/CNRS "Molécules et Cibles Thérapeutiques" Program.

References

(1) Sherr, C. J. Mammalian G1 Cyclins. *Cell* **1993**, *73*, 1059−1065.
(2) Morgan, D. Principles of Cdk regulation. *Nature* **1995**, *374*, 131−134.
(3) Pavletich, N. P. Mechanisms of cyclin-dependent kinase regulation: structures of Cdks, their cyclin activators, and Cip and INK4 inhibitors. *J. Mol. Biol.* **1999**, *287*, 821−828.
(4) Serrano, M.; Hannon, G. J.; Beach, D. A new regulatory motif in cell-cycle control causing specific inhibition of cyclinD/CDK4. *Nature* **1993**, *366*, 704−707.
(5) Kamb, A.; Gruis, N. A.; Weaver-Feldhaus, J.; Liu, Q.; Harshman, K.; Tavtigan, S. V.; Stockert, E.; Day, R. S.; Johnson, B. E.; Skolnick, M. H. A cell cycle regulator potentially involved in genesis of many tumor types. *Science* **1994**, *264*, 436−440.
(6) Nobori, T.; Miura, K.; Wu, D. J.; Lois, A.; Takabayashi, K.; Darson, D. A. Deletions of the cyclin-dependent kinase-4 inhibitor gene in multiple human cancers. *Nature* **1994**, *368*, 753−756.
(7) Levine, A. J. p53, the cellular gatekeeper for growth and division. *Cell* **1997**, *88*, 323−331.
(8) Hunter, T.; Pines, J. Cyclins and cancer II: CyclinD and CDK inhibitors come of age. *Cell* **1994**, *79*, 573−583.
(9) Sherr, C. J. Cancer cell cycles. *Science* **1996**, *274*, 1672−1677.
(10) Sausville, E. A. Complexities in the development of cyclin-dependent kinase inhibitor drugs. *Trends Mol. Med.* **2002**, *8*, S32−S37.
(11) Noble, M. E.; Endicott, J. A.; Johnson, L. N. Protein kinase inhibitors: Insights into drug design from structure. *Science* **2004**, *303*, 1800−1805.
(12) Dai, Y.; Grant, S. Small molecule inhibitors targeting cyclin-dependent kinases as anticancer agents. *Curr. Oncol. Rep.* **2004**, *6*, 123−130.
(13) Fischer, P. M.; Endicott, J.; Meijer, L. Cyclin-dependent kinase inhibitors. *Prog. Cell Cycle Res.* **2003**, *5*, 235−248.
(14) Knockaert, M.; Greengard, P.; Meijer, L. Pharmacological inhibitors of cyclin-dependent kinases. *Trends Pharmacol. Sci.* **2002**, *23*, 417−425.
(15) Meijer, L.; Raymond, E. Roscovitine and other purines as kinase inhibitors. From starfish oocytes to clinical trials. *Acc. Chem. Res.* **2003**, *36*, 417−425.
(16) Schulze-Gahmen, U.; Kim, S.-H. Structural basis for CDK6 activation by a virus-encoded cyclin. *Nat. Struct. Biol.* **2002**, *9*, 177−181.
(17) Taylor, S. S.; Radzio-Andzelm, E. Three protein kinase structures define a common motif. *Structure* **1994**, *2*, 345−355.
(18) Jeffrey, D. P.; Russo, A. A.; Polyak, K.; Gibbs, E.; Hurwitz, J. et al. Mechanism of CDK activation revealed by the structure of a cyclinA−CDK2 complex. *Nature* **1995**, *376*, 313−320.
(19) De Azevedo, W. F.; Leclerc, S.; Meijer, L.; Havlicek, L.; Strnad, M.; Kim, S.-H. Inhibition of cyclin-dependent kinases by purine analogues. *Eur. J. Biochem.* **1997**, *243*, 518−526.
(20) Sicheri, F.; Moarefi, I.; Kuriyan, J. Crystal structure of the Src family tyrosine kinase Hck. *Nature* **1997**, *385*, 602−609.
(21) Pettit, G. R. H.; M. S.; Doubek, D. L.; Schmidt, J. M.; Pettit, R. K.; Tackett, L. P. & Chapuis, J.-C. Antineoplastic agents 338. The cancer cell growth inhibitory constituents of *Terminalia arjuna* (Combretaceae). *J. Ethnopharmacol.* **1996**, *53*, 57−63.
(22) Schulze-Gahmen, U.; Kim, S.-H. Crystallization of a complex between human CDK6 and a virus-encoded cyclin is critically dependent on the addition of small charged organic molecules. *Acta Crystallogr., Sect. D: Biol. Crystallogr.* **2001**, *57*, 576−579.
(23) Otwinowski, Z.; Minor, W. Processing of X-ray diffraction data collected in oscillation mode. *Methods Enzymol.* **1997**, *276*, 307−326.
(24) Collaborative Computational Project, N. The CCP4 suite: programs for protein crystallography. *Acta Crystallogr., Sect. D: Biol. Crystallogr.* **1994**, *50*, 760−763.
(25) Brunger, A. T.; Adams, P. D.; Clore, G. M.; DeLano, W. L.; Grosse-Kunstleve, R. W. et al. Crystallography & NMR system: A new software suite for macromolecular structure determination. *Acta Crystallogr., Sect. D: Biol. Crystallogr.* **1998**, *54*, 905−921.
(26) Jones, T. A.; Zou, J. Y.; Cowan, S. W.; Kjelgaard, M. Improved methods for building protein models in electron density maps and the location of errors in these models. *Acta Crystallogr., Sect. A: Found. Crystallogr.* **1991**, *47*, 110−119.
(27) Sheriff, S.; Hendrickson, W. A.; Smith, J. L. Structure of myohemerythrin in the azidomet state at 1.7/1.3 Å resolution. *J. Mol. Biol.* **1987**, *197*, 273−296.
(28) Connolly, M. L. Analytical molecular surface calculation. *J. Appl. Crystallogr.* **1983**, *16*, 548−558.
(29) Rossman, M. G.; Argos, P. A. Comparison of the heme binding pocket in globins and cytochrome b5. *J. Biol. Chem.* **1975**, *250*, 7525−7532.
(30) Schulze-Gahmen, U.; De Bondt, H. L.; Kim, S.-H. High-resolution crystal structures of human cyclin-dependent kinase 2 with and without ATP: Bound waters and natural ligand as guides for inhibitor design. *J. Med. Chem.* **1996**, *39*, 4540−4546.
(31) Davies, T. G.; Bentley, J.; Arris, C. E.; Boyle, F. T.; Curtin, N. J. et al. Structure-based design of a potent purine-based cyclin-dependent inhibitor. *Nat. Struct. Biol.* **2002**, *9*, 745−749.

JM049353P